Anthracene-Tethered Ruthenium(II) Arene Complexes as Tools To Visualize the Cellular Localization of Putative Organometallic Anticancer Compounds

ARTICLE *in* INORGANIC CHEMISTRY · MARCH 2012

Impact Factor: 4.76 · DOI: 10.1021/ic202530j · Source: PubMed

Inorganic Chemistry

Article

pubs.acs.org/IC

Anthracene-Tethered Ruthenium(II) Arene Complexes as Tools To Visualize the Cellular Localization of Putative Organometallic Anticancer Compounds

Alexey A. Nazarov,*[,†] Julie Risse,[†] Wee Han Ang,[‡] Frederic Schmitt,[§] Olivier Zava,[†] Albert Ruggi,[†] Michael Groessl,[†] Rosario Scopelitti,[†] Lucienne Juillerat-Jeanneret,[§] Christian G. Hartinger,[⊥] and Paul J. Dyson*[,†]

[†]Institute of Chemical Sciences and Engineering, Swiss Federal Institute of Technology (EPFL), 1015 Lausanne, Switzerland

[‡]Department of Chemistry, National University of Singapore, Singapore 117543, Singapore

[§]University Institute of Pathology Centre Hospitalier Universitaire Vaudois (CHUV), 1011 Lausanne, Switzerland

[⊥]School of Chemical Sciences, The University of Auckland, Auckland 1142, New Zealand

Supporting Information

ABSTRACT: Anthracene derivatives of ruthenium(II) arene compounds with 1,3,5-triaza-7-phosphatricyclo[3.3.1.1]decane (pta) or a sugar phosphite ligand, viz., 3,5,6-bicyclophosphite-1,2-*O*-isopropylidene-α-D-glucofuranoside, were prepared in order to evaluate their anticancer properties compared to the parent compounds and to use them as models for intracellular visualization by fluorescence microscopy. Similar IC_{50} values were obtained in cell proliferation assays, and similar levels of uptake and accumulation were also established. The X-ray structure of [{Ru(η^6-$C_6H_5CH_2NHCO$-anthracene)Cl_2(pta)}] is also reported.

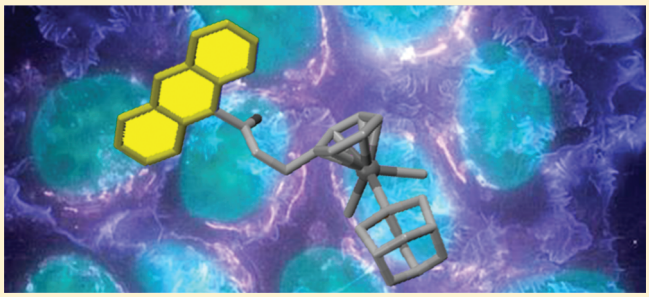

INTRODUCTION

Ruthenium-based antitumor drugs are being intensively studied, with two representatives currently undergoing clinical trials.[1−4] Many ruthenium compounds exhibit features that make them interesting for drug development including mild toxicity in vitro and high activity in in vivo models.[5−7] These biological effects may be attributed to a number of factors including selective accumulation in the tumor environment and/or tumor cells,[8−10] inhibition of the antimetastatic progression, and antiangiogenic properties.[7,11−13] It has also been shown that enzyme inhibition, as opposed to or in addition to covalent binding to DNA, may be responsible for these observed effects.[14−17]

Organoruthenium(II) arene compounds with 1,3,5-triaza-7-phosphatricyclo[3.3.1.1]decane (pta) coligands, termed RAPTA, and ethylene-1,2-diamine (en) ligands[18] have been studied extensively with respect to their tumor-inhibiting properties. In particular, the RAPTA scaffold has been functionalized with bioactive molecules.[1,19,20] One such modification entails substitution of the pta ligand with sugar-derived phosphites that might be able to preferentially accumulate in tumors because tumor cells have a high energy demand and a limited oxygen supply, leading to higher glucose uptake and glycolysis. Indeed, this modification resulted in compounds with enhanced in vitro anticancer activity against a panel of tumor cell lines and a high degree of selectivity for tumor cells over healthy cells.[10] The strategy of using sugar-based ligands to preferentially deliver metal drugs to tumors has been widely explored,[21] but definitive experiments demonstrating preferential uptake are lacking. Several attempts have been undertaken to localize metallodrugs in tumor cells, and different methods have been used.[22−31] However, in the case of ruthenium anticancer agents, the field is rather unexplored.[32,33] We describe herein functionalization of RAPTA-derived complexes with the anthracene fluorophore and an investigation of the antineoplastic activity and intracellular localization of the complexes with a pta ligand or a sugar-derived phosphite, in order to establish the role of the latter ligand in tumor uptake.

RESULTS AND DISCUSSION

Fluorescent analogues of RAPTA complexes and their carbohydrate derivatives were prepared by derivatization of the arene ring with anthracene via an amide bond to the piano-stool-configured ruthenium scaffold. Attachment of an anthracene moiety is expected to change the biological properties of the resulting derivative to a much lesser extent than other widely used fluorescent tags.[24,34−39] The synthetic route was adapted from an earlier report that describes the

Received: November 23, 2011
Published: March 6, 2012

preparation of RAPTA compounds carrying the glutathione-*S*-transferase inhibitor ethacrynic acid (EA).[14] 9-Anthracenecarboxylic acid was converted into its acid chloride by oxalyl chloride/*N*,*N*-dimethylformamide (DMF) and reacted with 1,4-cyclohexadiene-1-methylamine or 1,4-cyclohexadiene-1-ethylamine to yield *N*-(cyclohexa-1,4-dienylmethyl)anthracene-9-carboxamide and *N*-(2-(cyclohexa-1,4-dienyl)ethyl)anthracene-9-carboxamide, respectively. These cyclic dienes were reacted with $RuCl_3$ in ethanol under reflux to yield the respective Ru^{II}(arene) dimers as brown solids. Finally, the dimers were treated with 3,5,6-bicyclophosphite-1,2-*O*-isopropylidene-*α*-D-glucofuranoside or pta to yield complexes **1**−**4** (Scheme 1).

Scheme 1. Synthesis of 1−4 (a, 3,5,6-Bicyclophosphite-1,2-*O*-isopropylidene-*α*-D-glucofuranoside; b, 1,3,5-Triaza-7-phosphatricyclo[3.3.1.1]decane)

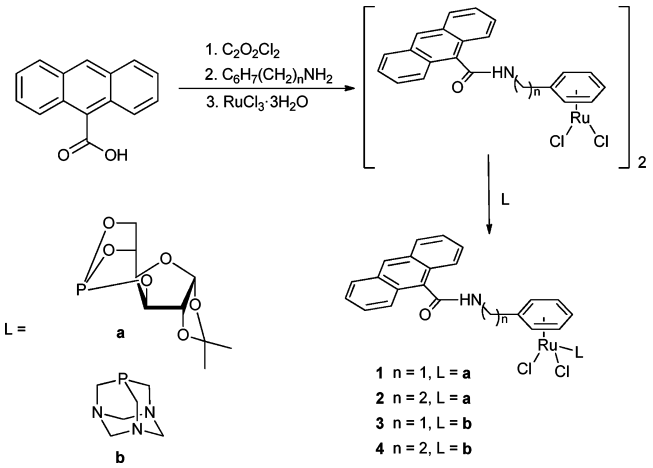

The compounds were characterized by ^1H, $^{13}C\{^1H\}$, and $^{31}P\{^1H\}$ NMR spectroscopy, mass spectrometry, and elemental analysis. $^{31}P\{^1H\}$ NMR spectroscopy was used to monitor the formation of complexes **1**−**4**. In these spectra, a shift from ca. 119 to 133 ppm and from −100 to −33 ppm was observed for the phosphite and pta ligands, respectively, upon coordination. In addition, characteristic shifts to lower frequency in both ^1H and $^{13}C\{^1H\}$ NMR spectra, as reported for similar types of complexes, were observed, confirming the proposed structure of the complexes.[10]

Single crystals of **3** suitable for X-ray diffraction analysis were obtained by slow diffusion of pentane into a chloroform solution containing the complex. Complex **3** features a piano-stool geometry (Figure 1) with bond lengths and angles similar to those of related RAPTA-C[40] and RAPTA-EA[14] complexes (Table 1). In the crystal, a combination of hydrogen bonding involving the pta ligands and *π*−*π*-stacking interactions between the anthracene units of adjacent molecules connects the molecules.

Complexes **1**−**4** undergo aquation in water via substitution of a chlorido ligand by an aqua group, as indicated by $^{31}P\{^1H\}$ NMR spectroscopy and consistent with studies on related compounds.[10] This transformation is characterized by a shift of the P atom resonance from approximately 133 to 140 ppm in the carbohydrate−phosphite complexes and from −33 to −28 ppm in the pta compounds. In addition, **1** and **2** undergo a P−O cleavage of the sugar phosphite carrier ligand in aqueous solution, as observed for structurally related ruthenium and osmium complexes.[10,43] Notably, neither ^1H nor $^{31}P\{^1H\}$ NMR

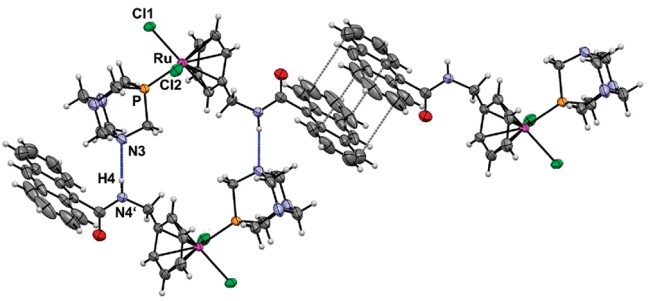

Figure 1. Molecular structure of **3**. The hydrogen-bonding network [N3···N4′ 3.000(1) Å] and *π*−*π*-stacking interactions [the shortest distance is 3.324(19) Å] are shown as solid and dashed lines, respectively. The ellipsoids are drawn at the 50% probability level.

Table 1. Comparison of the Bond Lengths (Å) and Angles (deg) of 3 with RAPTA-C and RAPTA-EA

	3	RAPTA-C	RAPTA-EA
Ru−arene$_{centroid}$ (Å)	1.691	1.701	1.697
Ru−P (Å)	2.2911(8)	2.296(2)	2.321(4)
Ru−Cl$_{aver}$ (Å)	2.415	2.421	2.429
Cl−Ru−Cl (deg)	88.84(3)	87.25(8)	89.32(11)
P−Ru−Cl1 (deg)	82.49(3)	83.42(8)	84.58(11)
P−Ru−Cl2 (deg)	86.31(3)	87.09(9)	82.09(12)

spectra suggest hydrolysis of the amide bond and the release of anthracene under the conditions, and therefore it is not unreasonable to assume that in in vitro studies the applied compounds enter the cells intact. Hydrolysis can be remarkably suppressed (>95%) by the addition of 100 mM NaCl.

The cytotoxicity of **1**−**4** was studied using MTT and [^{3}H]thymidine incorporation assays in 12 human cell lines comprising SW480, HT29, and CaCo2 colon carcinoma, MDA-MB231 and MCF-7 breast carcinoma, A549 lung carcinoma, A2780 and A2780cisR ovarian carcinoma, LN18, LN229, and LNZ308 glioblastoma, and HCEC cerebral endothelial cells (Table 2). Only **1** exhibited IC_{50} values lower than 200 *μ*M in the MTT assay, whereas the other complexes are basically nontoxic even after 72 h of drug exposure. Low in vitro cytotoxicities have been observed previously for structurally related compounds, and ruthenium compounds are, in general, less cytotoxic than the clinically established platinum compounds.[10] The $Ru^{II}(\eta^6$-*p*-cymene) compound with the same phosphorus-based ligand as that of **1** and **2** exhibited IC_{50} values in most cell lines in the range 360−680 *μ*M after 72 h of exposure. Incubation of SW480 and A549 cells for 96 h with the parent compound of **3** and **4**, i.e., RAPTA-C, showed no significant cytotoxicity with IC_{50} values of 170 and >640 *μ*M,[41] similar to the mentioned sugar derivative in SW480 (361 *μ*M).[10] Such behavior is often observed for ruthenium anticancer agents, and high cytotoxicity is not a prerequisite for antitumor activity in vivo or even in patients.[44,45] Moreover, carbohydrate complexes often exhibit low antineoproliferative activity in cell culture, which is accompanied by improved tolerability and only slightly lower antitumor activity in animal experiments.[21]

Tethering the anthracene moiety to the arene ligand did not significantly influence the in vitro antitumor activity, whereas the incorporation of conjugate *π* systems results in enhanced antitumor activity because of their intercalating properties and higher lipophilicities resulting in increased cellular uptake.[46] Because anthracene derivatives are known to exhibit intrinsic

dx.doi.org/10.1021/ic202530j | Inorg. Chem. 2012, 51, 3633−3639

Table 2. IC_{50} Values As Determined by the MTT Assay after 24, 48, and 72 h of Exposure of the Cells to 1−4 and RAPTA-C and by the [^{3}H]Thymidine Assay (Values in Parentheses As Measured after 24 h of Incubation with the Test Compound)

		$IC_{50}/\mu M$											
compound	cell line	LN18	LN229	LNZ308	SW480	HT29	CaCo2	A549	MDA-MB231	MCF-7	HCEC	A2780	A2780cisR
1	MTT, 24 h	>200	110	165	>200	>200	95	>200	>200	>200	>200	120	>200
	MTT, 48 h	90	40	140	70	100	40	>200	120	>200	60	35	40
	MTT, 72 h	50	70	200	80	120	125	>200	110	>200	50	30	>200
	[^{3}H]thym	(25)	(10)	(15)	(35)	(25)	(24)	(12)	(21)	(11)	(20)	(10)	(12)
2	MTT, 24 h	>200	>200	>200	>200	>200	>200	>200	>200	>200	>200	>200	>200
	MTT, 48 h	>200	100	>200	>200	>200	>200	>200	>200	>200	>200	>200	>200
	MTT, 72 h	>200	100	>200	>200	>200	>200	>200	>200	>200	>200	>200	>200
	[^{3}H]thym	(25)	(14)	(50)	(75)	(150)	(16)	(14)	(50)	(14)	(52)	(50)	(50)
3	MTT, 24 h	>200	>200	>200	>200	>200	>200	>200	>200	>200	>200	>200	>200
	MTT, 48 h	>200	>200	>200	>200	>200	>200	>200	>200	>200	>200	>200	>200
	MTT, 72 h	>200	>200	>200	>200	>200	>200	>200	>200	>200	>200	>200	>200
	[^{3}H]thym	(35)	(13)	(13)	(>200)	(>200)	(20)	(13)	(>200)	(14)	(18)	(35)	(>200)
4	MTT, 24 h	>200	>200	>200	>200	>200	>200	>200	>200	>200	>200	>200	>200
	MTT, 48 h	>200	>200	>200	>200	>200	>200	>200	>200	>200	>200	>200	>200
	MTT, 72 h	>200	>200	>200	>200	>200	>200	>200	>200	>200	>200	>200	>200
	[^{3}H]thym	(>200)	(>200)	(>200)	(>200)	(>200)	(50)	(>200)	(>200)	(25)	(>200)	(>200)	(>200)
RAPTA-C	MTT				170 ± 60[a]	436[b]		>1000[b]		>1000[b]			

[a]96 h (taken from ref 41). [b]72 h (taken from ref 42). LN18, LN229, and LNZ308: human glioblastoma cells. SW480, HT29, and CaCo2: human colon carcinoma cells. A549: human lung carcinoma cells. MDA-MB231 and MCF-7: human breast carcinoma cells. HCEC: human endothelial cells. A2780 and A2780cisR: human ovarian carcinoma cells, cisplatin-sensitive and resistant, respectively.

fluorescence, the compounds were thought to be suitable models for cellular uptake studies using fluorescence microscopy. Consequently, fluorescence emission spectra were recorded for **1** and **3**. Because of the relatively quick aquation of the compounds in aqueous solutions, the spectra were recorded in DMF. In both cases, the emission maxima were very similar at 412 and 411 nm, respectively (Figure 2).

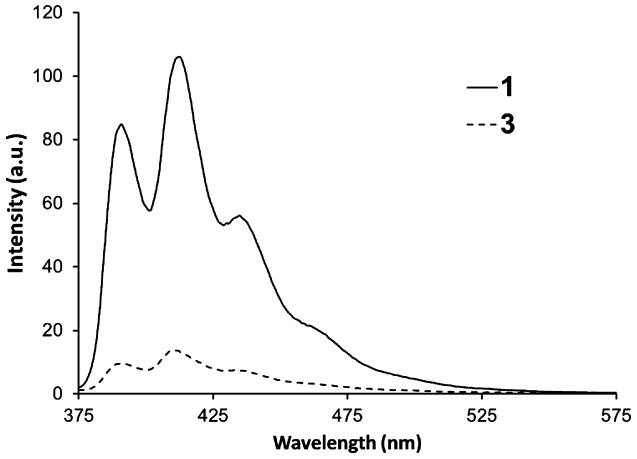

Figure 2. Fluorescence spectra of **1** and **3** (11 μM) after excitation at λ_{ex} = 365 nm.

However, the fluorescence intensity of **1** was much higher than that of **3**, demonstrating the influence of the phosphorus-derived ligands. This fact was also shown by determining the quantum yields of 0.126 and 0.036 for **1** and **3**.

Fluorescence microscopy was used to study the localization of the anthracene-functionalized compounds in A549 lung carcinoma cells in order to delineate the influence of the phosphorus ligand on the cellular visualization of the complexes. A549 lung carcinoma cells were incubated with **1** and **3** for 24 h at 50 μM (well below the cytotoxicity IC_{50}; Figure 3). Cells were fixed with a 4% buffered paraformaldehyde solution on a glass slide, and images were taken after excitation at 365 nm. Intense fluorescence was observed in the case of **1** with the sugar phosphite ligand, whereas only moderate fluorescence was detected for the pta complex **3** (ca. three times higher for **1**, resembling approximately the quantum yield ratio for both compounds), which is most

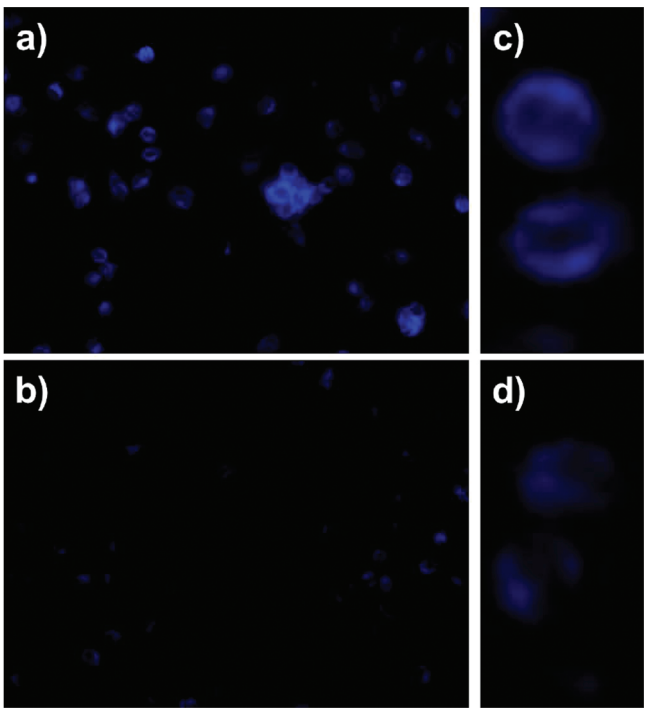

Figure 3. Fluorescence microscopy of A549 lung carcinoma cells treated with (a) **1** and (b) **3** (50 μM each) for 24 h (λ_{ex} 365 nm). (c and d) 6-fold-magnified zoom images of cells shown in a) and b), respectively.

dx.doi.org/10.1021/ic202530j | Inorg. Chem. 2012, 51, 3633−3639

probably related to the, in general, lower fluorescence emission of **3**. It appears that neither **1** nor **3** accumulate in the nucleus, as was observed by other methods with structurally related complexes.[33]

In order to elucidate the influence of the phosphorus-containing ligands on the cellular accumulation of anthracene-tethered Ru^{II}(arene) complexes, the ruthenium concentration was measured after incubation of A2780 cells with **1** and **3**. Very similar amounts of ruthenium were found after treatment with **1** and **3** at equimolar concentrations (332 ± 16 and 305 ± 48 pmol/10^6 cells of ruthenium, respectively). This is in the same dimension as that observed for the ruthenium compounds KP1019 and NAMI-A.[33] These data sets reveal only a minor influence of the phosphorus ligand on the uptake, which, however, might be leveled by the high lipophilicity related to the anthracene substituent.

In addition to the MTT assay, [^{3}H]thymidine incorporation was studied as a measure of the DNA synthesis as a function of the compound concentration. In this experimental setup, **1** was found to be the most inhibitory of the test compounds, followed by **2** and **3**. In contrast, **4** showed no activity against the majority of the human tumor cell lines, with the exception of the MCF-7 and CaCo2 cell lines. Compound **1** was similarly potent in all cell lines, with IC_{50} values in the range 10−35 μM and LN229 and MCF-7 representing the most sensitive cell lines. Interestingly, the MCF-7 cell line showed no sensitivity to the test compounds under the MTT assay conditions but was the most sensitive cell line in the [^{3}H]thymidine incorporation experiments.

■ CONCLUSIONS

In conclusion, we have prepared and characterized a series of fluorescent Ru^{II}(arene) complexes tethered with an anthracene moiety bearing pta or a sugar phosphite ligand with the aiming of assessing the relative cellular uptake of compounds. Cells incubated with the complex carrying the carbohydrate−phosphite ligand exhibited higher fluorescence intensities than those with pta because of the differences in the quantum yields of the complexes and, importantly, reveal that the complexes do not accumulate in the cell nucleus. No influence of the P-ligand on the cellular accumulation was observed, which might be related to the lipophilicity of the molecules.

■ EXPERIMENTAL SECTION

All solvents were purified and degassed prior to use.[47] ^{1}H, ^{13}C{^{1}H}, and ^{31}P{^{1}H} NMR spectra were recorded on a Bruker Avance II 400 spectrometer at room temperature and were referenced to the ^{1}H signal of the NMR solvent or to H_3PO_4 as an external reference for ^{31}P{^{1}H} NMR spectroscopy. Electrospray ionization mass spectra (ESI-MS) of the compounds were obtained in MeOH on a ThermoFinnigan LCQ Deca XP Plus quadrupole ion-trap instrument operated in positive-ion mode over a mass range of m/z 150−1000. The ionization energy was set at 3.5 kV and the capillary temperature at 150 °C. Melting points were determined with a Stuart Scientific SMP3 apparatus and are uncorrected. The flash chromatography system Varian 971-FP was used for purification. Elemental analyses were carried out by the microanalytical laboratory at EPFL (Table 3).

***N*-(Cyclohexa-1,4-dienylmethyl)anthracene-9-carboxamide.** A solution of anthracene-9-carbonyl chloride[48] (5.53 g, 23.0 mmol) in CH_2Cl_2 (60 mL) was added dropwise to a stirred solution of 1,4-cyclohexadiene-1-methanamine[49] (2.7 mL, 23.6 mmol) and triethylamine (4.1 mL, 29.5 mmol) in CH_2Cl_2 (120 mL). The reaction mixture was stirred for 12 h at room temperature. The solvent was evaporated, and the semicrystalline solid was suspended in toluene (25 mL). Triethylamine hydrochloride was removed by filtration and washed with toluene (3 × 5 mL), toluene was removed under reduced pressure, and the crude product was purified by column chromatography [eluent: *n*-hexane/EtAc (3:1)]. Yield: 3.31 g (54%). Mp: 152−153 °C. Elem anal. Calcd for $C_{22}H_{19}NO$: C, 84.31; H, 6.11; N, 4.47. Found: C, 84.22; H, 5.97; N, 4.23. ^{1}H NMR (400.13 MHz, $CDCl_3$): δ 8.50 (s, 1H, H_{ant}), 8.11 (d, J = 8.2 Hz, 2H, H_{ant}), 8.03 (d, J = 8.2 Hz, 2H, H_{ant}), 7.53 (m, 4H, H_{ant}), 6.06 (br s, 1H, NH), 5.76 (m, 3H, C=CH, CH=CH), 4.27 (d, J = 5.6 Hz, 2H, CH_2NH), 2.84 (m, 2H, CH_2), 2.75 (m, 2H, CH_2). ^{13}C{^{1}H} NMR (100.63 MHz, $CDCl_3$): δ 169.7 (CO), 131.9 (C_{diene}), 131.4 (C_{ant}), 130.9 (C_{ant}), 128.4 (C_{ant}), 128.1 (C_{ant}), 127.9 (C_{ant}), 126.5 (C_{ant}), 126.4 (C_{ant}), 125.0 (C_{ant}), 124.0 (C_{diene}), 123.7 (C_{diene}), 121.4 (C_{diene}), 45.5 ($NHCH_2$), 27.5 (C_{diene}), 26.5 (C_{diene}). MS (ESI$^+$): m/z 314 ([M + H]$^+$).

***N*-[2-(Cyclohexa-1,4-dienyl)ethyl]anthracene-9-carboxamide.** *N*-[2-(Cyclohexa-1,4-dienyl)ethyl]anthracene-9-carboxamide was obtained from anthracene-9-carbonyl chloride (5.53 g, 23.0 mmol), 1,4-cyclohexadiene-1-ethylamine[50] (3 mL, 23.6 mmol), and triethylamine (4.1 mL, 29.5 mmol) using the procedure described for *N*-(cyclohexa-1,4-dienylmethyl)anthracene-9-carboxamide. Yield: 3.17 g (42%). Mp: 173−176 °C. Elem anal. Calcd for $C_{23}H_{21}NO$: C, 84.37; H, 6.46; N, 4.28. Found: C, 84.30; H, 6.13; N, 4.41. ^{1}H NMR (400.13 MHz, $CDCl_3$): δ 8.49 (s, 1H, H_{ant}), 8.09 (d, J = 8.2 Hz, 2H, H_{ant}), 8.02 (d, J = 8.2 Hz, 2H, H_{ant}), 7.50 (m, 4H, H_{ant}), 6.04 (br s, 1H, NH), 5.75 (m, 2H, CH=CH), 5.56 (s, 1H, C=CH), 3.87 (m, 2H, $NHCH_2$), 2.75 (m, 2H, CH_2), 2.68 (m, 2H, CH_2), 2.43 (t, J = 6.2 Hz, 2H, $NHCH_2CH_2$). ^{13}C{^{1}H} NMR (100.63 MHz, $CDCl_3$): δ 169.5 (CO), 132.0 (C_{diene}), 131.6 (C_{ant}), 131.1 (C_{ant}), 128.3 (C_{ant}), 128.1 (C_{ant}), 128.0 (C_{ant}), 126.7 (C_{ant}), 125.5 (C_{ant}), 125.0 (C_{ant}), 124.1 (cyclohexadiene), 124.0 (C_{diene}), 121.6 (C_{diene}), 37.4 ($NHCH_2CH_2$), 37.3 ($NHCH_2CH_2$), 28.4 (CH_2), 26.7 (CH_2). MS (ESI$^+$): m/z 328 ([M + H]$^+$).

Bis[dichlorido(η^6-*N*-benzylanthracene-9-carboxamide)-ruthenium(II)]. A solution of *N*-(cyclohexa-1,4-dienylmethyl)-anthracene-9-carboxamide (2.0 g, 6.3 mmol) in degassed ethanol (150 mL) was added to ruthenium(III) chloride hydrate (0.55 g, 2.1

Table 3. Crystal Data and Structure Refinement for 3

empirical formula	$C_{28}H_{29}Cl_2N_4OPRu$
fw	640.49
temperature (K)	140(2)
wavelength (Å)	0.710 73
cryst syst	monoclinic
space group	$P2_1/c$
unit cell dimens	a = 17.1875(4) Å, α = 90°
	b = 12.9255(3) Å, β = 93.548(2)°
	c = 13.7320(4) Å, γ = 90°
volume (Å^3)	3044.80(13)
Z	4
density (calcd) (mg/m^3)	1.397
abs coeff (mm^{-1})	0.769
F(000)	1304
cryst size (mm^3)	0.34 × 0.26 × 0.21
θ range for data collection (deg)	2.85−28.41
index ranges	$-22 \le h \le 22$, $-17 \le k \le 17$, $-16 \le l \le 16$
reflns collected	21233
indep reflns	6641 [R(int) = 0.0273]
completeness to θ = 25.00°	95.2%
abs corrn	semiempirical from equivalents
max and min transmn	1.00000 and 0.87796
refinement method	full-matrix least squares on F^2
data/restraints/param	6641/0/334
GOF on F^2	1.068
final R indices [$I > 2\sigma(I)$]	R1 = 0.0380, wR2 = 0.1062
R indices (all data)	R1 = 0.0512, wR2 = 0.1122
largest diff peak and hole (e/Å^3)	0.845 and −0.587

dx.doi.org/10.1021/ic202530j | Inorg. Chem. 2012, 51, 3633−3639

mmol). The reaction mixture was refluxed at 90 °C for 10 h under a nitrogen atmosphere. Upon completion, a brown solid has formed, which was filtered, washed with ethanol (3 × 5 mL) and diethyl ether (2 × 5 mL), and dried in vacuo. Yield: 1.0 g (97%). Mp: >200 °C (dec). Elem anal. Calcd for $C_{44}H_{34}N_2O_2Ru_2Cl_4$: C, 54.67; H, 3.55; N, 2.90. Found: C, 54.64; H, 3.74; N, 3.11. ^{1}H NMR (400.13 MHz, DMSO-d_6): δ 9.40 (t, J = 5.6 Hz, 1H, NH), 8.69 (s, 1H, H_{ant}), 8.14 (m, 2H, H_{ant}), 7.88 (m, 2H, H_{ant}), 7.55 (m, 4H, H_{ant}), 6.19 (m, 2H, H_{Ar}), 6.07 (m, 2H, H_{Ar}), 5.91 (m, 1H, H_{Ar}), 4.53 (d, J = 5.6 Hz, 2H, NHCH_2). ^{13}C{^{1}H} NMR (100.63 MHz, DMSO-d_6): δ 169.3 (CO), 132.6 (C_{ant}), 131.0 (C_{ant}), 128.9 (C_{ant}), 128.1 (C_{ant}), 127.8 (C_{ant}), 127.2 (C_{ant}), 126.1 (C_{ant}), 125.4 (C_{ant}), 102.2 (C_{Ar}), 89.2 (C_{Ar}), 86.7 (C_{Ar}), 85.2 (C_{Ar}), 41.8 ($NHCH_2$). MS (ESI$^+$): m/z 990 ([M + Na]$^+$).

Bis[dichlorido(η^6-*N*-phenethylanthracene-9-carboxamide)-ruthenium(II)]. This compound was obtained from *N*-(2-(cyclohexa-1,4-dienyl)ethyl)anthracene-9-carboxamide (1.0 g, 3.1 mmol) and ruthenium(III) chloride hydrate (0.27 g, 1.0 mmol) using the procedure described for bis[dichlorido(η^6-*N*-benzylanthracene-9-carboxamide)ruthenium(II)]. Yield: 0.57 g (96%). Mp: >200 °C (dec). Elem anal. Calcd for $C_{46}H_{38}N_2O_2Ru_2Cl_4$: C, 55.54; H, 3.85; N, 2.81. Found: C, 55.76; H, 4.07; N, 2.92. ^{1}H NMR (400.13 MHz, DMSO-d_6): δ 8.94 (t, J = 5.2 Hz, 1H, NH), 8.65 (s, 1H, H_{ant}), 8.12 (m, 2H, H_{ant}), 7.74 (m, 2H, H_{ant}), 7.54 (m, 4H, H_{ant}), 6.09 (m, 2H, H_{Ar}), 5.92 (d, J = 5.9 Hz, 2H, H_{Ar}), 5.86 (m, 1H, H_{Ar}), 3.89 (m, 2H, NHCH_2CH$_2$), 2.82 (t, J = 6.3 Hz, 2H, NHCH$_2$CH_2). ^{13}C{^{1}H} NMR (100.63 MHz, DMSO-d_6): δ 168.6 (CO), 133.5 (C_{ant}), 131.1 (C_{ant}), 128.8 (C_{ant}), 127.7 (C_{ant}), 127.6 (C_{ant}), 126.9 (C_{ant}), 126.0 (C_{ant}), 125.7 (C_{ant}), 105.0 (C_{Ar}), 88.9 (C_{Ar}), 86.6 (C_{Ar}), 84.4 (C_{Ar}), 39.1 ($NHCH_2CH_2$), 33.0 ($NHCH_2CH_2$). MS (ESI$^+$): m/z 462 ([M − 2Cl]$^{2+}$).

[Dichlorido(η^6-*N*-benzylanthracene-9-carboxamide)(3,5,6-bicyclophosphite-1,2-*O*-isopropylidene-α-D-glucofuranoside)-ruthenium(II)] (1). A solution of 3,5,6-bicyclophosphite-1,2-*O*-isopropylidene-α-D-glucofuranoside (51 mg, 0.2 mmol) in dichloromethane (20 mL) was added to a suspension of [{Ru(η^6-$C_6H_5CH_2NHCO$-anthracene)Cl_2}$_2$] (100 mg, 0.1 mmol) in dichloromethane (20 mL), under nitrogen. The reaction mixture was stirred for 12 h at room temperature, and the progress was monitored by ^{31}P{^{1}H} NMR specroscopy. The reaction mixture was concentrated undervacuum, and diethyl ether was added to precipitate the product, which was isolated by filtration and washed with diethyl ether (3 × 5 mL). The crude product was purified by short column chromatography [CH_2Cl_2/MeOH (10:1)]. Yield: 93 mg (62%). Mp: >220 °C (dec). Elem anal. Calcd for $C_{31}H_{30}NO_7PRuCl_2{\cdot}0.5CH_2Cl_2$: C, 48.88; H, 4.04; N, 1.81. Found: C, 49.14; H, 4.11; N, 2.01. ^{1}H NMR (400.13 MHz, $CDCl_3$): δ 8.53 (s, H_{ant}), 8.08 (d, J = 8.4 Hz, 2H, H_{ant}), 8.05 (d, J = 8.4 Hz, 2H, H_{ant}), 7.56 (m, 4H, H_{ant}), 7.20 (br, 1H, NH), 5.98 (m, 5H, H-1, H_{Ar}), 5.53 (br s, 1H, H_{Ar}), 4.96 (m, 2H, NHCH_2), 4.77 (m, 1H, H_5), 4.48 (s, 1H, H_3), 4.39 (s, 1H, H_2), 4.06 (m, 2H, H-4, H_6), 3.86 (br, 1H, $H_{6'}$), 1.46 (s, 3H, CH_3), 1.30 (s, 3H, CH_3). ^{13}C{^{1}H} NMR (100.63 MHz, $CDCl_3$): δ 170.2 (CO), 130.9 (C_{ant}), 130.5 (C_{ant}), 128.8 (C_{ant}), 128.7 (C_{ant}), 128.0 (C_{ant}), 127.2 (C_{ant}), 125.6 (C_{ant}), 124.7 (C_{ant}), 112.4 ($C(CH_3)_2$), 106.8 (C_{Ar}), 105.5 (C_1), 92.3 (C_{Ar}), 91.9 (C_{Ar}), 89.2 (C_{Ar}), 88.2 (C_{Ar}), 84.1 (C_{Ar}), 83.4 (C-3), 79.1 (C_2), 77.2 (C_4), 74.6 (C_5), 69.3 (C_6), 40.7 ($NHCH_2$), 26.8 (CH_3), 26.2 (CH_3). ^{31}P{^{1}H} NMR (161.98 MHz, $CDCl_3$): δ 133.2. MS (ESI$^+$): m/z 696 ([M − Cl]$^+$).

[Dichlorido(η^6-*N*-phenethylanthracene-9-carboxamide)-(3,5,6-bicyclophosphite-1,2-*O*-isopropylidene-α-D-glucofuranoside)ruthenium(II)] (2). Complex **2** was obtained from 3,5,6-bicyclophosphite-1,2-*O*-isopropylidene-α-D-glucofuranoside (50 mg, 0.2 mmol) and [{Ru(η^6-$C_6H_5CH_2CH_2NHCO$-anthracene)Cl_2}$_2$] (100 mg, 0.1 mmol) using the procedure described for **1**. Yield: 100 mg (67%). Mp: >220 °C (dec). Elem anal. Calcd for $C_{32}H_{32}NO_7PRuCl_2{\cdot}0.25CH_2Cl_2$: C, 50.52; H, 4.27; N, 1.83. Found: C, 50.25; H, 4.14; N, 1.73. ^{1}H NMR (400.13 MHz, $CDCl_3$, 25 °C): δ 8.46 (s, 1H, H_{ant}), 7.99 (d, J = 8.3 Hz, 2H, H_{ant}), 7.94 (d, J = 8.3 Hz, 2H, H_{ant}), 7.49 (m, 4H, H_{ant}), 6.69 (br s, 1H, NH), 6.17 (d, J = 3.4 Hz, 1H, H_1), 5.82 (m, 4H, H_{Ar}), 5.60 (m, 1H, H_{Ar}), 4.99 (m, 1H, H_5), 4.75 (m, 1H, H_3), 4.72 (d, J = 3.4 Hz, 1H, H_2), 4.36 (dd, J = 12.4 and 9.6 Hz, 1H, H_6), 4.25 (s, 1H, H_4), 4.15 (m, 1H, $H_{6'}$), 4.09 (m, 2H, NHCH_2CH$_2$), 3.07 (t, J = 6.7 Hz, 2H, NHCH$_2$CH_2), 1.49 (s, 3H, CH_3), 1.33 (s, 3H, CH_3). ^{13}C{^{1}H} NMR (100.63 MHz, $CDCl_3$, 25 °C): δ 169.7 (CO), 131.4 (C_{ant}), 131.0 (C_{ant}), 128.5 (C_{ant}), 128.3 C_{ant}), 127.9 (C_{ant}), 126.8 (C_{ant}), 125.5 C_{ant}), 125.0 (C_{ant}), 112.5 ($C(CH_3)_2$), 110.6 (C_{Ar}), 105.6 (C_1), 91.4 (C_{Ar}), 90.1 (C_{Ar}), 89.6 (C_{Ar}), 83.6 (C_2, CAr), 77.2 (C_4), 74.7 (C_5), 69.4 (C_6), 38.7 ($NHCH_2CH_2$), 33.1 ($NHCH_2CH$), 26.8 (CH_3), 26.2 (CH_3). ^{31}P{^{1}H} NMR (161.98 MHz, $CDCl_3$, 25 °C): δ 133.9. MS (ESI$^+$): m/z 711 ([M − Cl]$^+$), 768 ([M + Na]$^+$).

[Dichlorido(η^6-*N*-benzylanthracene-9-carboxamide)(1,3,5-triaza-7-phosphaadamantane)ruthenium(II)] (3). Complex **3** was obtained from 1,3,5-triaza-7-phosphaadamantane (32 mg, 0.2 mmol) and [{Ru(η^6-$C_6H_5CH_2NHCO$-anthracene)Cl_2}$_2$] (100 mg, 0.1 mmol) using the procedure described for **1**. Yield: 60 mg (44.7%). Mp: >220 °C (dec). Elem anal. Calcd for $C_{28}H_{29}N_4OPRuCl_2{\cdot}0.8CH_2Cl_2$: C, 48.83; H, 4.35; N, 7.90. Found: C, 48.55; H, 4.45; N, 7.73. ^{1}H NMR (400.13 MHz, DMF-d_7): δ 8.89 (1H, H_{ant}), 8.34 (m, 2H, H_{ant}), 8.21 (m, 2H, H_{ant}), 7.75 (m, 4H, H_{ant}), 6.24 (s, 4H, H_{Ar}), 5.71 (s, 1H, H_{Ar}), 4.79 (d, J = 5.8 Hz, 2H, NHCH_2), 4.73 (s, 6H, NCH_2N), 4.58 (s, 6H, PCH_2N). ^{13}C{^{1}H} NMR (100.63 MHz, DMF-d_7): δ 169.4 (CO), 133.0 (C_{ant}), 131.4 (C_{ant}), 128.7 (C_{ant}), 128.0 (C_{ant}), 127.9 (C_{ant}), 126.8 (C_{ant}), 125.8 (C_{ant}), 125.4 (C_{ant}), 103.7 (C_{Ar}), 87.9 (C_{Ar}), 87.1 (C_{Ar}), 79.3 (C_{Ar}), 72.8 (J = 6.6 Hz, NCH_2N), 52.6 (J = 17.8 Hz, PCH_2), 41.8 (CH_2NH). ^{31}P{^{1}H} NMR (161.98 MHz, DMF-d_7): δ −32.1. MS (ESI$^+$): m/z 663 ([M + Na]$^+$).

[Dichlorido(η^6-*N*-phenethylanthracene-9-carboxamide)-(1,3,5-triaza-7-phosphaadamantane)ruthenium(II)] (4). Complex **4** was obtained from 1,3,5-triaza-7-phosphaadamantane (33 mg, 0.2 mmol) and [{Ru(η^6-$C_6H_5CH_2CH_2NHCO$-anthracene)Cl_2}$_2$] (100 mg, 0.1 mmol) using the procedure described for **1**. Yield: 65 mg (48.8%). Mp: >220 °C (dec). Elem anal. Calcd for $C_{29}H_{31}N_4OPRuCl_2{\cdot}0.25CH_2Cl_2$: C, 51.99; H, 4.70; N, 8.29. Found: C, 51.65; H, 4.47; N, 8.45. ^{1}H NMR (400.13 MHz, DMSO-d_6): δ 8.92 (t, J = 5.1 Hz, 1H, NH), 8.65 (s, 1H, H_{ant}), 8.12 (d, J = 7.9 Hz, 2H, H_{ant}), 7.74 (d, J = 7.9 Hz, 2H, H_{ant}), 7.53 (m, 4H, H_{ant}), 5.88 (m, 2H, H_{Ar}), 5.75 (m, 2H, H_{Ar}), 5.44 (m, 1H, H_{Ar}), 4.44 (s, 6H, NCH_2N), 4.21 (s, 6H, PCH_2N), 3.85 (m, 2H, NHCH_2CH$_2$), 2.67 (t, J = 6.4 Hz, 2H, NHCH$_2$CH_2). ^{13}C{^{1}H} NMR (100.63 MHz, DMSO-d_6): δ 168.6 (CO), 133.6 (C_{ant}), 131.1 (C_{ant}), 128.5 (C_{ant}), 127.7 (C_{ant}), 127.4 (C_{ant}), 126.4 (C_{ant}), 125.6 (C_{ant}), 106.7 (C_{Ar}), 88.2 (C_{Ar}), 86.3 (C_{Ar}), 78.5 (C_{Ar}), 72.7 (J = 6.6 Hz, NCH_2N), 52.4 (J = 17.8 Hz, PCH_2N), 39.1 ($NHCH_2CH_2$), 33.1 ($NHCH_2CH_2$). ^{31}P{^{1}H} NMR (161.98 MHz, DMSO-d_6): δ −31.4. MS (ESI$^+$): m/z 619 ([M − Cl]$^+$).

Hydrolysis. Samples were dissolved in H_2O/D_2O/DMSO (8:1:1) at 25 °C. For investigation on the effect of the chloride ion concentration on the ligand exchange, sodium chloride (100 mM) was added to the solution and samples were analyzed by ^{31}P{^{1}H} NMR spectroscopy.

Cellular Accumulation of Ruthenium. Cells were seeded in six-well plates and incubated with the corresponding complex at a concentration of 50 μM for 5 h. At the end of the incubation period, the cells were rinsed twice with 2.0 mL of PBS, detached by adding 0.5 mL of an enzyme-free cell dissociation solution (Millipore, Switzerland), and collected by centrifugation. All samples were digested in ICP-MS-grade concentrated nitric acid (Sigma Aldrich, Switzerland) for 3 h at room temperature and filled to a total volume of 8.0 mL with ultrapure water. Indium was added as an internal standard at a concentration of 0.5 ppb. The metal contents were determined using an Elan DRC II ICP-MS (Perkin-Elmer, Switzerland) equipped with a Meinhard nebulizer and a cyclonic spray chamber. The ICP mass spectrometer was tuned daily using a solution provided by the manufacturer containing 1 ppb of each magnesium, indium, cesium, barium, tin, and uranium. External standards were prepared gravimetrically from single element standards (CPI International, Amsterdam, The Netherlands), using identical acid and internal standard concentrations.

Fluorescence Spectroscopy. Fluorescence measurements were performed on a Varian Cary Eclipse spectrofluorimeter at room temperature. Solutions **1** and **3** were prepared in DMF (11 μM). The

dx.doi.org/10.1021/ic202530j | Inorg. Chem. 2012, 51, 3633−3639

fluorescence spectra of **1** and **3** were recorded 30 min after sample preparation (λ_{ex} = 365 nm; slit width of 5 nm). Quantum yields (Φ) were determined by comparing the wavelength-integrated intensities (I or I_R) of isoabsorptive diluted solutions (Abs < 0.1) with reference to anthracene (Φ_R = 1.27 in ethanol) by the equation[51]

$$\Phi = \Phi_R \frac{n^2 I}{n_R{}^2 I_R}$$

where n and n_R are the refractive index of the sample and reference solvent, respectively.

Cell Lines and Culture Conditions. Human A2780 and A2780cisR ovarian carcinoma cell lines were obtained from the European Centre of Cell Cultures (ECACC, Porton Down, Salisbury, U.K.). Human SW480, HT29, and CaCo2 colon carcinoma, MDA-MB231 and MCF-7 breast carcinoma, and A549 lung carcinoma cells were obtained from the American Type Culture Collection, human cerebral endothelial cells (HCEC) were a kind gift of D. Staminirovic and A. Muruganandam, Ottawa, Canada, LN18, LN229, and LNZ308 glioblastoma cells were obtained from AC Diserens Neurosurgery Service, CHUV, Lausanne, Switzerland. These cells are routinely grown in Dulbecco's Modified Eagle Medium containing 4.5 g/L glucose and glutamax and were supplemented with 10% heat-inactivated fetal bovine serum and antibiotics. Cultures were maintained at 37 °C in a humidified atmosphere containing 6% CO_2. All cell culture reagents were purchased from Gibco-BRL, Basel, Switzerland.

Determination of the Cell Viability and DNA Synthesis. For these experiments, cells were grown in 48-well plates (Costar, Integra Biosciences, Cambridge, MA) as monolayers for 24 h in a complete medium with 10% fetal calf serum (FCS) to reach subconfluence. Then a fresh complete medium with 5% FCS was added together with the drugs, and the culture was continued for another 72 h. The compounds were predissolved at 20 mM in DMSO and then added to the cell culture medium at the required concentration with a maximum DMSO content of 0.5% (v/v) to be incubated for 24, 48, or 72 h. At these concentrations, DMSO has no effect on the cell viability and synthesis of DNA.

The cell viability was determined using the MTT assay, which quantifies the mitochondrial activity in metabolically active cells, essentially as reported previously. Briefly, following drug exposure, MTT (Sigma, final concentration 0.2 mg/mL) was added to the cell culture medium for the final 2 h, and then the culture medium was aspirated and the violet formazan precipitate dissolved in 0.1 M HCl in 2-propanol. The optical density, which is directly proportional to the number of surviving cells, was quantified at 540 nm using a multiwell plate reader (iEMS Reader MF, Labsystems, USA), and the percentage of surviving cells was calculated from the absorbance of untreated cells.

Thymidine incorporation was used to assess the DNA synthesis essentially as previously described.[52] Briefly, following drug exposure, 1 μCi/mL [^{3}H]thymidine (Amersham Pharmacia, Dübendorf, Switzerland) was added to the cell culture medium for the last 2 h, and incorporation was quantified in a β-counter (Rackbeta, LKB) after precipitation with 10% trichloracetic acid and dissolution in 0.1% sodium dodecylsulfate in 0.1 M NaOH. Experiments were performed in triplicate. The amount of viable cells and of DNA synthesis was calculated as the ratio of the absorbance or CPM of treated to untreated cells, and IC_{50} values were calculated from dose–response curves.

Determination of Cell-Associated Drug Fluorescence by Fluorescence Microscopy. Cells were grown on histological slides in a complete medium, exposed to the ruthenium compounds (50 μM) for 24 h, and fixed for 15 min at 4 °C in a 4% buffered paraformaldehyde solution. After washing, the slides were rehydrated and analyzed under a fluorescence microscope (Axioplan2, Carl Zeiss, Feldbach, Switzerland) with the filters set at 365 nm excitation wavelength (BP 365/12, FT 395, and LP 397). The intensity of the fluorescence was compared using ImageJ (1.42q).

■ ASSOCIATED CONTENT

Ⓢ Supporting Information

Crystallographic data for the structural analysis of **3**. This material is available free of charge via the Internet at http://pubs.acs.org. The atomic coordinates for this structure have also been deposited with the Cambridge Crystallographic Data Centre as CCDC 854958. The coordinates can be obtained, on request, from the Director, Cambridge Crystallographic Data Centre, 12 Union Road, Cambridge CB2 1EZ, U.K.

■ AUTHOR INFORMATION

Corresponding Author

*E-mail: alexey.nazarov@epfl.ch (A.A.N.), paul.dyson@epfl.ch (P.J.D.). Tel: +41-21-6939854. Fax: +41-21-6939780.

Notes

The authors declare no competing financial interest.

■ ACKNOWLEDGMENTS

The authors are grateful to the Swiss National Science Foundation, National Centre of Competence in Research "Chemical Biology–Visualisation and Control of Biological Processes Using Chemistry", COST D39, and EPFL for financial support. This research was supported by a Marie Curie Intra European Fellowship within the 7th European Community Framework Programme (Project 220890-SuRuCo to A.A.N.).

■ REFERENCES

(1) Hartinger, C. G.; Dyson, P. J. *Chem. Soc. Rev.* **2009**, *38*, 391–401.
(2) van Rijt, S. H.; Sadler, P. J. *Drug Discovery Today* **2009**, *14*, 1089–1097.
(3) Gasser, G.; Ott, I.; Metzler-Nolte, N. *J. Med. Chem.* **2011**, *54*, 3–25.
(4) Hartinger, C. G.; Phillips, A. D.; Nazarov, A. A. *Curr. Top. Med. Chem.* **2011**, *11*, 2688–2700.
(5) Alessio, E.; Mestroni, G.; Bergamo, A.; Sava, G. *Curr. Top. Med. Chem.* **2004**, *4*, 1525–1535.
(6) Kapitza, S.; Jakupec, M. A.; Uhl, M.; Keppler, B. K.; Marian, B. *Cancer Lett.* **2005**, *226*, 115–121.
(7) Scolaro, C.; Bergamo, A.; Brescacin, L.; Delfino, R.; Cocchietto, M.; Laurenczy, G.; Geldbach, T. J.; Sava, G.; Dyson, P. J. *J. Med. Chem.* **2005**, *48*, 4161–4171.
(8) Hartinger, C. G.; Zorbas-Seifried, S.; Jakupec, M. A.; Kynast, B.; Zorbas, H.; Keppler, B. K. *J. Inorg. Biochem.* **2006**, *100*, 891–904.
(9) Khalaila, I.; Bergamo, A.; Bussy, F.; Sava, G.; Dyson, P. J. *Int. J. Oncol.* **2006**, *29*, 261–268.
(10) Berger, I.; Hanif, M.; Nazarov, A. A.; Hartinger, C. G.; John, R. O.; Kuznetsov, M. L.; Groessl, M.; Schmitt, F.; Zava, O.; Biba, F.; Arion, V. B.; Galanski, M.; Jakupec, M. A.; Juillerat-Jeanneret, L.; Dyson, P. J.; Keppler, B. K. *Chem.—Eur. J.* **2008**, *14*, 9046–9057.
(11) Vacca, A.; Bruno, M.; Boccarelli, A.; Coluccia, M.; Ribatti, D.; Bergamo, A.; Garbisa, S.; Sartor, L.; Sava, G. *Br. J. Cancer* **2002**, *86*, 993–998.
(12) Rademaker-Lakhai, J. M.; Van Den Bongard, D.; Pluim, D.; Beijnen, J. H.; Schellens, J. H. M. *Clin. Cancer Res.* **2004**, *10*, 3717–3727.
(13) Nowak-Sliwinska, P.; van Beijnum, J. R.; Casini, A.; Nazarov, A. A.; Wagnières, G.; van den Bergh, H.; Dyson, P. J.; Griffioen, A. W. *J. Med. Chem.* **2011**, *54*, 3895–3902.
(14) Ang, W. H.; Parker, L. J.; De Luca, A.; Juillerat-Jeanneret, L.; Morton, C. J.; Lo Bello, M.; Parker, M. W.; Dyson, P. J. *Angew. Chem.* **2009**, *121*, 3912–3915.
(15) Pizarro, A. M.; Sadler, P. J. *Biochimie* **2009**, *91*, 1198–1211.
(16) Novakova, O.; Nazarov, A. A.; Hartinger, C. G.; Keppler, B. K.; Brabec, V. *Biochem. Pharmacol.* **2009**, *77*, 364–374.

(17) Wu, B.; Ong, M. S.; Groessl, M.; Adhireksan, Z.; Hartinger, C. G.; Dyson, P. J.; Davey, C. A. *Chem.—Eur. J.* **2011**, *17*, 3562−3566.
(18) Farrer, N. J.; Sadler, P. J. Medicinal inorganic chemistry: state of the art, new trends, and a vision of the future. In *Bioinorganic Medicinal Chemistry*; Alessio, E., Ed.; Wiley-VCH: Weinheim, Germany, 2011; pp 1−47.
(19) Johansson, K.; Ito, M.; Schophuizen, C. M. S.; Thengumtharayil, S. M.; Heuser, V. D.; Zhang, J.; Shimoji, M.; Vahter, M.; Ang, W. H.; Dyson, P. J.; Shibata, A.; Shuto, S.; Ito, Y.; Abe, H.; Morgenstern, R. *Mol. Pharm.* **2011**, *8*, 1698−1708.
(20) Tan, Y. Q.; Dyson, P. J.; Ang, W. H. *Organometallics* **2011**, *30*, 5965−5971.
(21) Hartinger, C. G.; Nazarov, A. A.; Ashraf, S. M.; Dyson, P. J.; Keppler, B. K. *Curr. Med. Chem.* **2008**, *15*, 2574−2591.
(22) Meijera, C.; van, L. M. J. A.; Nienhuis, E. F.; Blom, N.; Mulder, N. H.; de, V. E. G. E. *Biochem. Pharmacol.* **2001**, *61*, 573−578.
(23) Salem, K. A.; Szymanski-Exner, A.; Lazebnik, R. S.; Breen, M. S.; Gao, J.; Wilson, D. L. *IEEE Trans. Med. Imaging* **2002**, *21*, 1310-6.
(24) Kalayda, G. V.; Zhang, G.; Abraham, T.; Tanke, H. J.; Reedijk, J. *J. Med. Chem.* **2005**, *48*, 5191−5202.
(25) Björn, E.; Nygren, Y.; Thi Nhu Nguyen, T. T.; Ericson, C.; Nöjd, M.; Naredi, P. *Anal. Biochem.* **2007**, *363*, 135−142.
(26) Brouwers, E. E. M.; Tibben, M.; Rosing, H.; Schellens, J. H. M.; Beijnen, J. H. *Mass Spectrom. Rev.* **2008**, *27*, 67−100.
(27) Hall, M. D.; Okabe, M.; Shen, D. W.; Liang, X. J.; Gottesman, M. M. *Annu. Rev. Pharmacol. Toxicol.* **2008**, *48*, 495−535.
(28) Sanchez-Cano, C.; Hannon, M. J. *Dalton Trans.* **2009**, 10765−10773.
(29) Esteban-Fernandez, D.; Moreno-Gordaliza, E.; Canas, B.; Palacios, M. A.; Gomez-Gomez, M. M. *Metallomics* **2010**, *2*, 19−38.
(30) Benedetti, B. T.; Peterson, E. J.; Kabolizadeh, P.; Martinez, A.; Kipping, R.; Farrell, N. P. *Mol. Pharm.* **2011**, *8*, 940−948.
(31) Aitken, J. B.; Levina, A.; Lay, P. A. *Curr. Top. Med. Chem.* **2011**, *11*, 553−571.
(32) Zava, O.; Zakeeruddin, S. M.; Danelon, C.; Vogel, H.; Grätzel, M.; Dyson, P. J. *ChemBioChem* **2009**, *10*, 1796−1800.
(33) Groessl, M.; Zava, O.; Dyson, P. J. *Metallomics* **2011**, *3*, 591−599.
(34) Barragán, E.; Gordillo, B.; Vargas, G.; Cortez, M. T.; Jaramillo, B. E.; Villa-Treviño, S.; Fattel-Fazenda, S.; Ortega, J.; Velazco, L. *Arkivoc* **2005**, *2005*, 436−448.
(35) Kapp, T.; Müller, S.; Gust, R. *ChemMedChem* **2006**, *1*, 560−564.
(36) Zobi, F.; Mood, B. B.; Wood, P. A.; Fabbiani, F. P. A.; Parsons, S.; Sadler, P. J. *Eur. J. Inorg. Chem.* **2007**, 2783−2796.
(37) Marqués-Gallego, P.; Den Dulk, H.; Brouwer, J.; Kooijman, H.; Spek, A. L.; Roubeau, O.; Teat, S. J.; Reedijk, J. *Inorg. Chem.* **2008**, *47*, 11171−11179.
(38) Wilson, J. J.; Fedoce Lopes, J.; Lippard, S. J. *Inorg. Chem.* **2010**, *49*, 5303−5315.
(39) Wu, S.; Wang, X.; Zhu, C.; Song, Y.; Wang, J.; Li, Y.; Guo, Z. *Dalton Trans.* **2011**, *40*, 10376−10382.
(40) Allardyce, C. S.; Dyson, P. J.; Ellis, D. J.; Heath, S. L. *Chem. Commun.* **2001**, 1396−1397.
(41) Hanif, M.; Nazarov, A. A.; Legin, A.; Groessl, M.; Arion, V. B.; Jakupec, M. A.; Tsybin, Y. O.; Dyson, P. J.; Keppler, B. K.; Hartinger, C. G. *Chem. Commun.* **2012**, *48*, 1475−1477.
(42) Ang, W. H.; Daldini, E.; Scolaro, C.; Scopelliti, R.; Juillerat-Jeannerat, L.; Dyson, P. J. *Inorg. Chem.* **2006**, *45*, 9006−9013.
(43) Hanif, M.; Nazarov, A. A.; Hartinger, C. G.; Kandioller, W.; Jakupec, M. A.; Arion, V. B.; Dyson, P. J.; Keppler, B. K. *Dalton Trans.* **2010**, *39*, 7345−7352.
(44) Bergamo, A.; Sava, G. *Dalton Trans.* **2011**, *40*, 7817−7823.
(45) Jakupec, M. A.; Galanski, M.; Arion, V. B.; Hartinger, C. G.; Keppler, B. K. *Dalton Trans.* **2008**, 183−194.
(46) Aird, R. E.; Cummings, J.; Ritchie, A. A.; Muir, M.; Morris, R. E.; Chen, H.; Sadler, P. J.; Jodrell, D. I. *Br. J. Cancer* **2002**, *86*, 1652−1657.
(47) Armarego, W. L. F.; Chai, C. *Purification of Laboratory Chemicals*, 5th ed.; Butterworth-Heinemann: Oxford, 2003; p 608.
(48) Adams, H.; Hunter, C. A.; Lawson, K. R.; Perkins, J.; Spey, S. E.; Urch, C. J.; Sanderson, J. M. *Chem.—Eur. J.* **2001**, *7*, 4863−4877.
(49) Ang, W. H.; Daldini, E.; Juillerat-Jeanneret, L.; Dyson, P. J. *Inorg. Chem.* **2007**, *46*, 9048−9050.
(50) Crabb, T. A.; Wilkinson, J. R. *J. Chem. Soc., Perkin Trans. 1* **1975**, 1465−1470.
(51) Montalti, M.; Credi, A.; Prodi, L.; Gandolfi, M. T. *Handbook of Photochemistry*, 3rd ed.; CRC Press: Boca Raton, FL, 2006.
(52) Juillerat-Jeanneret, L.; Bernasconi, C. C.; Bricod, C.; Gros, S.; Trepey, S.; Benhattar, J.; Janzer, R. C. *Cancer Invest.* **2008**, *26*, 597−609.